Geometric Effects in an Elastic Tensegrity Structure

I. J. Oppenheim (ijo@andrew.cmu.edu)
Depts. of Civil and Environmental Engineering and Architecture, Carnegie Mellon University

W. O. Williams (wow@cmu.edu)
Dept. of Mathematical Sciences, Carnegie Mellon University

Abstract. Tensegrity structures are under-constrained, three-dimensional, self-stressing structural systems. They demonstrate an infinitesimal flex and when loaded they display a nonlinear geometric stiffening. In earlier work many examples of the resulting force-displacement relationship have been demonstrated numerically, and some aspects of the force-displacement relationship have been derived analytically. In this article an energy formulation is presented for the case of a simple but representative tensegrity structure, yielding an exact solution for the force-displacement relationship. The solution makes understandable the different appearance of the force-displacement relationship when comparing a system at zero prestress to one at high prestress, or when comparing a system with almost-inextensible members to one with highly extensible members. The exact solution also is offered as a benchmark against which numerical solutions should be tested. Furthermore, the formulation and the solution reveal conditions of asymmetry of response that have not been noted previously.

Keywords: tensegrity, structural stability, elastic structures

AMS Subject Classification: 52C25, 70B10, 70B15, 73K05

1. Introduction

1.1. A Basic Tensegrity Structure

Following the pattern of sculptures by Kenneth Snelson in 1948, in 1961 Buckminster Fuller patented a class of cable-bar assemblages which he called tensegrity structures. Figure 1 pictures a well-known example of such a structure constructed with three bars and six cables. Tensegrity structures have attracted interest recently because of their potential advantages as lightweight structures, as variable geometry trusses, as shape adaptive structures, and as deployable structures. The structure pictured represents fully the distinctive features of tensegrity structures.

It is a form-finding structure, an under-constrained structural system, prestressible while displaying an infinitesimal flexure even when the constituent elements are undeformable. It forms only at nodal geometries in which the statics matrix becomes rank deficient. The

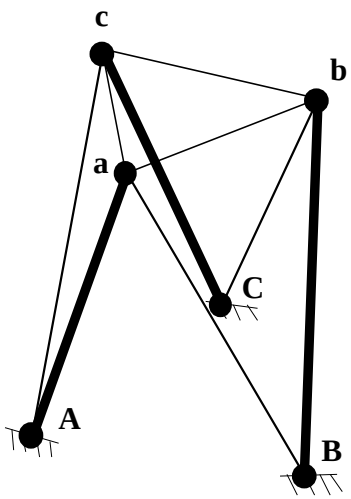

Figure 1. Simple Tensegrity Structure

mechanics of the structure at that equilibrium geometry, in the absence of external loads, is treated in various sources and will not be repeated here. The general principles of the equilibrium mechanics [1, 10, 9, 14] are based on the properties of the statics matrix and apply only in an infinitesimal neighborhood of the equilibrium geometry. Those principles have been discussed in application to this particular tensegrity structure [7], an equilibrium analysis of this same structure can be found within a comprehensive text on under-constrained structures [5], and this same example has been treated in a recent article [4] that addresses questions of nonlinear response and control.

If constructed with 9 rigid bars, at a generic nodal geometry, a truss with the topology of Figure 1 would be a statically determinate rigid body. It would neither admit a prestress nor admit any nodal movement whatsoever. As a consequence, if any bar were replaced by a cable, the position would become unstable. However, at a tensegrity geometry such a structure admits a prestress and also displays an infinitesimal flexure, that is, a infinitesimal nodal displacement which does not require lengths of the structural elements to change. The prestress places six of the bars in tension, allowing them to be replaced by cables, as shown in Figure 1, without affecting either the infinitesimal flexibility or the stability. Greater (finite) nodal movement then is observed to require some cable elongation but no cable shortening, thereby explaining physically why the equilibrium position is a stable one.

In an actual tensegrity structure constructed with almost-inextensible members (such as steel cables) the infinitesimal flex is plainly evident

(and consists in a simultaneous rotation and elevation change of the upper triangle). Following the nomenclature of [5], nodal loadings in the direction of the infinitesimal flex are termed perturbation loads, and nodal loadings orthogonal thereto are termed equilibrium loads. While equilibrium loads can be resolved directly by statics, resolution of perturbation loads requires nodal displacements, mobilizing the (nonlinear) geometric stiffening. The main contribution of this article is the derivation and examination of an exact solution for the geometric stiffening, the nonlinear force-displacement relationship displayed by the tensegrity structure when subject to perturbational loadings.

In the case just described the geometric stiffening effect is pronounced. In the close vicinity of the equilibrium geometry the structure is quite soft, but the stiffness increases dramatically with finite, but relatively small, displacement. However, we note that many laboratory examples are purposely constructed using highly extensible members such as rubber cords, because such assemblies allow both graceful form-finding and easy demonstration of shape changing. In such cases it may be difficult, from casual observation, to distinguish the infinitesimal flex and its nonlinear geometric stiffening from the large nodal displacements resulting from elastic effects. Nonetheless, analyzing any response to nodal forces requires the inclusion of the nonlinear geometric stiffening effect.

Characterization of tensegrity positions of an arbitrary assemblage of bars and cables is a difficult problem (*cf.* [14]). Here we shall be concerned with the behavior of our structure from an established tensegrity position.

1.2. The Tensegrity Position and Motions

The problem will be examined for a tensegrity structure as pictured in Figure 1, further simplified by assumptions of symmetry and uniformity. The structure is taken as a right regular prism, in which the end faces are equilateral triangles, perpendicular to the axis joining their centroids. The tensegrity position, shown in [2] to be globally unique, then is known to require a $5\pi/6$ relative rotation between the triangles.

The three bars are assumed to be rigid, and the three cables comprising the edges of the end face inextensible, while the three diagonal cables are linearly elastic with equal moduli. Any applied force will be required to be symmetric about the axis of the prism. The result of these simplifications is that the triangular faces remain parallel and centered on the z-axis, so that all nodal displacements can be described by the angle of relative rotation or by the concomitant vertical displacement.

The infinitesimal flexure of the system is an infinitesimal rotation of the upper triangle about its axis.

1.3. Force-Displacement Relations: Previous Work

It has been observed that the initial stiffness in the direction of the infinitesimal flex depends upon the prestress; that if the system is assembled without prestress then the initial stiffness would be zero, whereas prestress creates an initial stiffness proportionate in magnitude. It is also understood that the stiffness increases as the structure is displaced along the direction of flex. This effect is of practical interest. In some instances the variation in stiffness with displacement is a feature that may prove useful in controlling the compliance of a structure and in controlling vibration (*cf.* [8]). Therefore, several investigators have addressed the question of generating the nonlinear force-displacement relationship resulting when such a structure is subjected to perturbation loads.

In principle, performing such analyses numerically should be fairly straightforward. Systematic methods have been outlined [5, 9] for doing so in general. Skelton and coworkers in [12, 13] present extensive results for structures with multi-stage topology. Within that work they arrive at equations of motion relating nodal forces and nodal displacements by using a Lagrangian formulation and show, in [11], numerically generated plots, recording such force-displacement relationships. Similar numerical analysis is contained in work recently described by Murakami [6] and by Motro and others [4] describing multi-stage variants of structures based upon the topology depicted in Figure 1. The authors [7] have shown results obtained using a commercial finite element analysis package, applied to a structure with almost-inextensible members. Those numerical results show the initial stiffening effect of prestress and then the dramatic geometric stiffening effect with displacement.

2. Kinematics, Elasticity and Equilibrium

We consider the structure shown in Figure 1. The nodes A, B, and C are pinned to ground, the legs Aa, Bb, and Cc are inextensible bars, the elements ab, bc, and ca are inextensible cables, while the cross-cables Ac, Ba, and Cb are taken to be linearly elastic. Considering only the cross-cables as elastic simplifies the calculations, but captures the essence of the elastic response of such systems.

Because of the inextensibility, the upper triangle moves as a rigid body, and hence its position is easily described by the location of one point and a rotation matrix. We assume here that

– The triangles ABC and abc are congruent equilateral triangles.

– The legs have the same length, L.

– The cross-cables are identical in length and in elastic modulus.

As we will see, this complete symmetry leads to simple calculations.

We set the origin of coordinates at the centroid of the lower triangle, and locate its three vertices by the vectors $\mathbf{p}_A$, $\mathbf{p}_B$, and $\mathbf{p}_C$ in the $x-y$ plane; for definiteness, we take $\mathbf{p}_A = a\,\mathbf{i}$, to be directed in the x-coordinate direction. We take $\mathbf{x}$ to be the vector locating the centroid of the upper triangle, so that the locations of the upper points are given as

$$\begin{aligned} \mathbf{p}_a &= \mathbf{x} + Q\,\mathbf{p}_A, \\ \mathbf{p}_b &= \mathbf{x} + Q\,\mathbf{p}_B, \\ \mathbf{p}_c &= \mathbf{x} + Q\,\mathbf{p}_C, \end{aligned} \tag{2.1}$$

where Q is the rotation matrix. Because of the symmetry of our system we have that Q is a rotation of angle ϕ (counterclockwise) about the z-axis, and $\mathbf{x} = h\mathbf{k}$. Thus, for example,

$$\mathbf{p}_a = h\,\mathbf{k} + a\cos\phi\,\mathbf{i} - a\sin\phi\,\mathbf{j}. \tag{2.2}$$

The feasible range of ϕ is from $-\pi/3$, where the cross-cables interfere, to π, where the legs interfere.

Now the constraint that the legs are of fixed length L becomes

$$(\mathbf{p}_a - \mathbf{p}_A)^2 = (h\,\mathbf{k} + a(\cos\phi - 1)\,\mathbf{i} - a\sin\phi\,\mathbf{j})^2 = L^2 \tag{2.3}$$

or

$$h^2 = L^2 - 2a^2(1-\cos\phi). \tag{2.4}$$

Next, we calculate the length λ of each cross-cable from

$$\lambda^2 = (\mathbf{p}_c - \mathbf{p}_A)^2 = (h\,\mathbf{k} + Q\,\mathbf{p}_C - \mathbf{p}_A)^2, \tag{2.5}$$

and since $\mathbf{p}_C = a\left(-\frac{1}{2}\,\mathbf{i} + \frac{\sqrt{3}}{2}\,\mathbf{j}\right)$, we arrive at

$$\begin{aligned} \lambda^2 &= h^2 + 2a^2 + a^2(\cos\phi - \sqrt{3}\sin\phi) \\ &= L^2 + a^2(3\cos\phi - \sqrt{3}\sin\phi), \end{aligned} \tag{2.6}$$

where we have used (2.4). For later use, we calculate the derivatives:

$$2\lambda\,\lambda' = a^2(-3\sin\phi - \sqrt{3}\cos\phi), \tag{2.7}$$

$$2\lambda\,\lambda'' = a^2(\sqrt{3}\sin\phi - 3\cos\phi) - 2(\lambda')^2. \tag{2.8}$$

If k is the spring constant, and λ_N is the **natural length** of the cross-cables, then the total elastic energy is

$$U(\phi) = \frac{3}{2}k\left[(\lambda - \lambda_N)^2\right] \tag{2.9}$$

(when $\lambda \geq \lambda_N$; otherwise it is zero). The applied moment or torque associated to a rotation ϕ is then the derivative of the energy with respect to ϕ:

$$M(\phi) = U'(\phi) = 3k(\lambda - \lambda_N)\lambda'(\phi), \tag{2.10}$$

and the equilibria of the unloaded system occur when this is equal to zero. This occurs when $\lambda = \lambda_N$ or when $\lambda' = 0$. The latter occurs at

$$\phi = -\frac{\pi}{6} \quad \text{or} \quad \phi = \frac{5\pi}{6}\,. \tag{2.11}$$

We note that an increment in ϕ from either position results in an *infinitesimal flexure*, which neither lengthens nor shortens any bar or cable.

Continuing,

$$U''(\phi) = 3k\lambda(\phi)^2 - 3k(\lambda - \lambda_N)\lambda''(\phi), \tag{2.12}$$

and it is easy to see that the point $\phi = -\pi/6$ always yields a maximum of energy, so that we can disregard it. [1]

On the other hand $\phi = 5\pi/6$, the classical *tensegrity placement* for the symmetric structure, yields

$$U''(\frac{5\pi}{6}) = 3k\lambda'(\frac{5\pi}{6})^2 = 3\sqrt{3}ka^2(1 - \frac{\lambda_N}{\lambda_0}). \tag{2.13}$$

Here we have introduced the **equilibrium length** of the cross-cables:

$$\lambda_0 = \lambda(\frac{5\pi}{6}) = \sqrt{L^2 - 2\sqrt{3}a^2}\,. \tag{2.14}$$

If $\lambda_0 < \lambda_N$, then the cables would be fully slack in this placement, and it follows that the position is unstable [3]; henceforth, we assume that $\lambda_0 \geq \lambda_N$. If $\lambda_0 > \lambda_N$, the second derivative of the energy is positive, and we confirm that the tensegrity placement is a local minimum of the energy (and a minimum of the cross-cable length λ).

The point where $\lambda = \lambda_N$, if it is attainable and if it is not the tensegrity placement, corresponds to a position in which the structure has zero prestress and the cables may be further shortened by rotation.

[1] In fact, one can show that this position would require compression in the edges of the upper triangle, and hence it is not a tensegrity position.

This is unstable [3]. On the other hand, if $\lambda = \lambda_N$ *coincides* with the tensegrity placement, the cable cannot be further shortened by rotation. Both second and third derivatives of the energy are zero in this case, but the fourth derivative is positive, and hence this again is a local minimum of energy, confirming its stability. This corresponds to the case of zero pre-stress in the tensegrity placement.

3. Response to Applied Loads

To continue in a symmetric geometry, we can consider only symmetric loadings. For convenience, we re-express all functions in terms of the angular deflection θ away from the equilibrium placement:

$$\phi = \theta + \frac{5\pi}{6}. \tag{3.1}$$

We find

$$\lambda(\theta) = \sqrt{L^2 - 2\sqrt{3}a^2\cos\theta}, \tag{3.2}$$

and

$$M(\theta) = 3\sqrt{3}ka^2\left[1 - \frac{\lambda_N}{\lambda(\theta)}\right]\sin\theta. \tag{3.3}$$

Note that $M(\theta)$ is *anti-symmetric* about $\theta = 0$.

3.1. Applied Torque

Consider first an applied torque, generated, for example, by equal tangential loads applied at each vertex. The derivative of the torque-angle relation (3.3) is

$$M'(\theta) = 3\sqrt{3}\,k\,a^2\,\left(1 - \frac{\lambda_N}{\lambda}\right)\cos\theta + 9\,k\,a^4\,\left(\frac{\lambda_N}{\lambda^3}\right)\sin^2\theta, \tag{3.4}$$

and thus the initial modulus of the elastic response is

$$M'(0) = 3\sqrt{3}\,k\,a^2\,\left(1 - \frac{\lambda_N}{\lambda_0}\right) = 3\sqrt{3}a^2\left(\frac{k\,(\lambda_0 - \lambda_N)}{\lambda_0}\right). \tag{3.5}$$

Note that the modulus is a linear function of the prestress

$$k\,(\lambda_0 - \lambda_N), \tag{3.6}$$

so that, in particular, the initial modulus is zero if there is no prestress. The second derivative of the relation is

$$M''(\theta) \;=\; -\frac{9\,\lambda_N\,a^4\,(\sin(\theta))^3}{2\lambda(\theta)^{5/2}} + \frac{3\,\lambda_N\,a^2\sqrt{3}\sin(\theta)\cos(\theta)}{2\lambda(\theta)^{3/2}}$$

$$-\frac{1}{2}\left(1-\frac{\lambda_N}{\lambda(\theta)}\right)\sin(\theta) \tag{3.7}$$

which is zero at $\theta = 0$ regardless of the value of the prestress.

Figures 3–4 show plots of $M(\theta)$ for a structure with $L/a = 18/7$ for various choices of prestress (prestrains, $(\lambda_0 - \lambda_N)/\lambda_N$, from 0% to 300%). Figure 3 shows the response over a small range of rotations for zero prestress and for a small prestress (prestrain of 0.2%). Figure 4 shows the response under several prestresses over the feasible range $-7\pi/6 < \theta < \pi/6$. Note, in particular, that the curvature for small positive θ is negative for small prestresses, but positive for large prestresses, and for the latter the response appears much more nearly linear. The curvature sign-change occurs at a prestrain of

$$\frac{L + 6a^4 + 3\sqrt{3}L^2a^2}{L^4 - 12a^4}\,, \tag{3.8}$$

which in this geometry is 165%.

3.2. Vertical Loading

Another forcing which will produce a symmetric response is one whose resultant is a purely vertical loading at the centroid of the triangle *abc*. We consider the relation between the applied force and the height h of the triangle. Since h and ϕ are related by (2.4), we can find h as a function of θ as

$$h(\theta) = \sqrt{L^2 - a^2(2 + \sqrt{3}\cos\theta + \sin\theta)}. \tag{3.9}$$

This function is invertible in the feasible domain. Using (2.4) and (2.6), we can solve to find the elastic energy as a function of h; the derivative of this function with respect to h is the force F required to displace the triangle vertically. The resulting equations are not particularly enlightening. It is easier to express this force (taking it positive if directed downwards) in terms of θ as

$$\begin{aligned} F(\theta) &= -U'(\theta)\frac{d\theta}{dh} \\ &= M(\theta)/h'(\theta) \\ &= M(\theta)\left\{\frac{2h(\theta)}{a^2(\cos\theta - \sqrt{3}\sin\theta)}\right\}. \end{aligned} \tag{3.10}$$

This force must approach infinity as the derivative $h'(\theta)$ approaches zero, which occurs at $\theta = \pi/6$, the point where the legs interfere, and at $\theta = -5\pi/6$, the point where the legs are vertical.

Next we define the (downwards) displacement from the equilibrium position as

$$\delta(\theta) = h(0) - h(\theta) \tag{3.11}$$

and regard (3.10) and (3.11), using (3.9), as parametric equations describing the response function.

The derivatives of the force-displacement relation are calculated in these terms as

$$F'(h) = \frac{M'(\theta)}{h'(\theta)^2} - \frac{M(\theta)}{h'(\theta)^3}\left(h''(\theta)\right), \tag{3.12}$$

$$F''(h) = \frac{M''(\theta)}{h'(\theta)^3} - \frac{3M'(\theta)}{h'(\theta)^4} + M(\theta)\left[\frac{3h''(\theta)^2}{h'(\theta)^5} - \frac{h'''(\theta)}{h'(\theta)^4}\right]. \tag{3.13}$$

Evaluation at $\theta = 0$ gives the initial modulus and the initial curvature of the response as

$$F'(h_0) = -\frac{M'(0)}{h'(0)^2} = \frac{3\sqrt{3}}{h_0\lambda_0}k\,(\lambda_0 - \lambda_N), \tag{3.14}$$

$$F''(h_0) = -\frac{3M'(0)}{h'(0)^4} = -\frac{144\sqrt{3}\,{h_0}^4 k\,(\lambda_0 - \lambda_N)}{a^6\lambda_0}. \tag{3.15}$$

The initial modulus is zero if there is no prestress, and is linear in the prestress, as for the previous loading. The initial curvature of the response, however, now is zero only for null prestress, and otherwise is negative and proportional to the prestress.

Figures 5–7 are graphs of F versus δ for the same values of L and a and the same assortment of prestresses as in the previous calculations. Figure 5 shows the response over a small range of displacement for the cases of zero prestress and small prestress (prestrain of 0.2%). The next two figures show more distinctly the discrepancy between this response and the "perturbation" loading previously analysed. Figure 6 shows the response over a range of θ values from -0.8 to 0.3 for various prestresses. Finally, Figure 7 shows the response over the range of θ between the infinities of F, for the zero prestress and the highest prestress (300% prestrain). The responses for the other prestress values are trapped between these two.

3.3. Natural Mode Response

Finally, to relate the current calculations to those obtained using the structural-matrix approach, we may look at the direction of infinitesimal flexure of the structure. The direction of infinitesimal flexure is that in which the structure may move with no initial extension of any of its edges; this vector is the null vector of the transpose of the structural

matrix. Of course, once the structure is forced out of the tensegrity placement by an imposed force, this direction is no longer defined. To model what might be meant by a finite "displacement in the direction of the natural mode", we shall consider the path of a node of our structure in the continued symmetric deformation. We will calculate *the relation between arc-length along this path and the corresponding force directed tangential to that path*. The tangent vector to that path at the equilibrium position is the direction of infinitesimal flexure, and the corresponding force the initial forcing needed in that direction to drive the deformation.

As a function of the angle ϕ of rotation, the position of node a is given by

$$\mathbf{p}_a(\phi) = h(\phi)\,\mathbf{k} + a\cos\phi\,\mathbf{i} - a\sin\phi\,\mathbf{j}, \tag{3.16}$$

where $h(\phi)$ is given by (2.4). Its derivative is

$$\mathbf{p}_a'(\phi) = a\left[-\frac{a\sin\phi}{h(\phi)}\,\mathbf{k} - \sin\phi\,\mathbf{i} - \cos\phi\,\mathbf{j}\right], \tag{3.17}$$

which has squared length

$$a^2 + \frac{a^4}{h(\phi)^2}\sin^2\phi. \tag{3.18}$$

Thus the arc-length along the curve is

$$s(\phi) = a\int_{5\pi/6}^{\phi}\sqrt{1 + \frac{a^4}{h(\phi)^2}\sin^2\phi}\,d\phi, \tag{3.19}$$

and we can, in principle, invert this to determine ϕ in terms of s. Then we could express the elastic energy in terms of s; its derivative with respect to s is the magnitude T of the tangential force required to drive the deformation. In this way we find

$$T(\phi) = \frac{M(\phi)}{a\sqrt{1 + \frac{a^4}{h(\phi)^2}\sin^2\phi}}. \tag{3.20}$$

Finally, we can express both T and s in term of the rotation-past-equilibrium θ. As before, we use this parameterization to plot the relation of T and s.

Figure 8 shows the response for the geometry already used, for various prestresses, verifying that the response in this mode is essentially the same as the torque-rotation response.

4. Remarks

The response of tensegrity structures has been observed to show a geometric stiffening, and we have found an analytic demonstration verifying this behavior, despite our assumption that the elastic elements are linear in response for all extensions. We hope that this solution may be useful, in particular, as a benchmark for development of numerical analysis of tensegrity structures.

The torque-rotation relation describes the fundamental response of the system. As we have noted, the initial modulus is linear in the prestress, and, since the initial value of the second derivative is zero regardless of the prestress, the graph shows an initially cubic behavior. The geometric non-linearization of response clearly is more pronounced for lower values of the prestress; for higher values the linear term dominates within the small-deformation range of motion. There is even a change in values of curvature near equilibrium (always zero *at* equilibrium) from negative to positive as the prestress becomes large. The departure from the upwards curvature form of response occurs at values of prestress which would be obtainable only in materials which could tolerate very large extensions (for the geometry we use for the plots, 165% strain) ; with metal cross-cables, for example, it would not be observable in practice.

As we have noted, the system may allow large rotations in the "unwinding" direction (θ negative), and the torque reaches a maximum, which can be calculated from (3.4). It is interesting that this occurs *before* the point where the cross cables are at maximum length (the point of maximum energy). As the unwinding continues, the geometry of the truss begins to allow the torque to be exercised more efficiently in counteracting the elastic forces. Continuing, one arrives at the point where the cross-cables are at their maximum length and the torque is zero. This is a point of unstable equilibrium.

It can be seen that the torque-angle loading and the natural mode loading yield essentially the same response. The natural-mode loading effects the torquing of the structure with no extraneous "equilibrium" loading, in contrast to the vertical loading or an $x - y$ plane loading.

The vertical loading response presumably is more typical of the response of an tensegrity structure to an arbitrary applied force. The force-displacement relation is clearly distinguished from that of the natural mode loading. To begin, the response is not symmetric about zero, as in the other cases. And, although the same sort of prestress-initial modulus relation and non-linear response occur as in the other cases, the stiffening is much more pronounced under this loading, due to the geometric relation prescribed by the constraints. There is also a

distinct difference in the curvature of the response for small values of displacement. Finally, we note the approach to infinity of the response shown in Figure 7 is related to, but not directly caused by, the approach to physical interference of the structural elements.

This analysis is interestingly similar to that of a well-known model problem (*cf.*[1]). The system shown in Figure 2 is an under-constrained prestressible system..

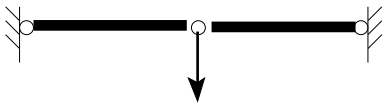

Figure 2. Two-dim. Model

When the nodes are colinear a prestress state is possible and an infinitesimal flex is present. If the distance between the supports is $2\,L$, the natural length of each bar is L_N, and each bar has a spring constant of k, then it is easy to see that the force required to displace the central node by a distance x is

$$2\,k\,(1-\frac{L_N}{\sqrt{L^2+x^2}})\,x. \tag{4.1}$$

The response shows a geometric stiffening effect, asymptotic to a linear graph. The small displacement approximation to (4.1) is

$$2k\left(1-\frac{L_N}{L}\right)x+\frac{kL_N}{L^3}x^3+o(x^5), \tag{4.2}$$

verifying that the initial modulus is zero if the system is not prestressed, but proportional to the prestress if it exists. Our results for natural-mode loading for our tensegrity structure are remarkably similar to (4.1).

References

1. Calladine, C. R.: 1978, 'Buckminster Fuller's "Tensegrity" strutures and Clerk Maxwell's rules for the construction of stiff frames'. *Int. J. Solids Struct.* **14**, 161–172.
2. Connelly, R. and M. Terrell: 1995, 'Globally rigid symmetric tensegrities'. *Structural Topology* **21**, 59–78.
3. Connelly, R. and W. Whiteley: 1996, 'Second-order rigidity and prestress stability for tensegrity frameworks'. *SIAM J. Discrete Math.* **9**, 453–491.
4. Djouadi, S., R. Motro, J. C. Pons, and B. Crosnier: 1998, 'Active Control of Tensegrity Systems'. *J. Aerospace Eng.* **11**, 37–44.
5. Kuznetsov, E. N.: 1991, *Underconstrained Structural Systems.* New York: Springer Verlag.

6. Murakami, H., Y. Nishimura, T. J. Impelluso, and R. E. Skelton: 1998, 'A Virtual Reality-Based CAD System for Tensegrity Structures'. In: *Proc. 12th Engineering Mechanics Conference*, Vol. 9. pp. 197–200.
7. Oppenheim, I. J. and W. O. Williams: 1997, 'Tensegrity Prisms as Adaptive Structures'. In: *Proc. Symp. Adaptive Structures and Material Systems*. pp. 113–120.
8. Oppenheim, I. J. and W. O. Williams: 1998, 'Vibration effects in a tensegrity prism'. In: *Proc. 12th Engineering Mech. Conf.* pp. 28–31.
9. Pellegrino, S.: 1990, 'Analysis of prestressed mechanisms'. *Int. J. Solids and Structures* **26**, 1329–1350.
10. Pellegrino, S. and C. R. Calladine: 1986, 'Matrix analysis of statically and kinematically indeterminate frameworks'. *Int. J. Solids Structures* **22**, 409–428.
11. Skelton, R. E. and R. Adhikari: 1998, 'An Introduction to Smart Tensegrity Structures'. In: *Proc. 12th Engineering Mechanics Conference*. pp. 24–27.
12. Skelton, R. E. and C. Sultan: 1997, 'Controllable tensegrity, a new class of smart structures'. In: V. V. Varadan and J. Chandra (eds.): *Smart Materials and Structures*, Vol. 3039. pp. 166–177.
13. Sultan, C. and R. E. Skelton: 1997, 'Integrated Design of Controllable Tensegrity Structures'. In: *Adaptive Structures and Material Systems*, Vol. 54. pp. 27–36.
14. Whiteley, W.: 1997, 'Tensegrity Frameworks'. In: H. Crapo and W. Whiteley (eds.): *The Geometry of Rigid Structures*.

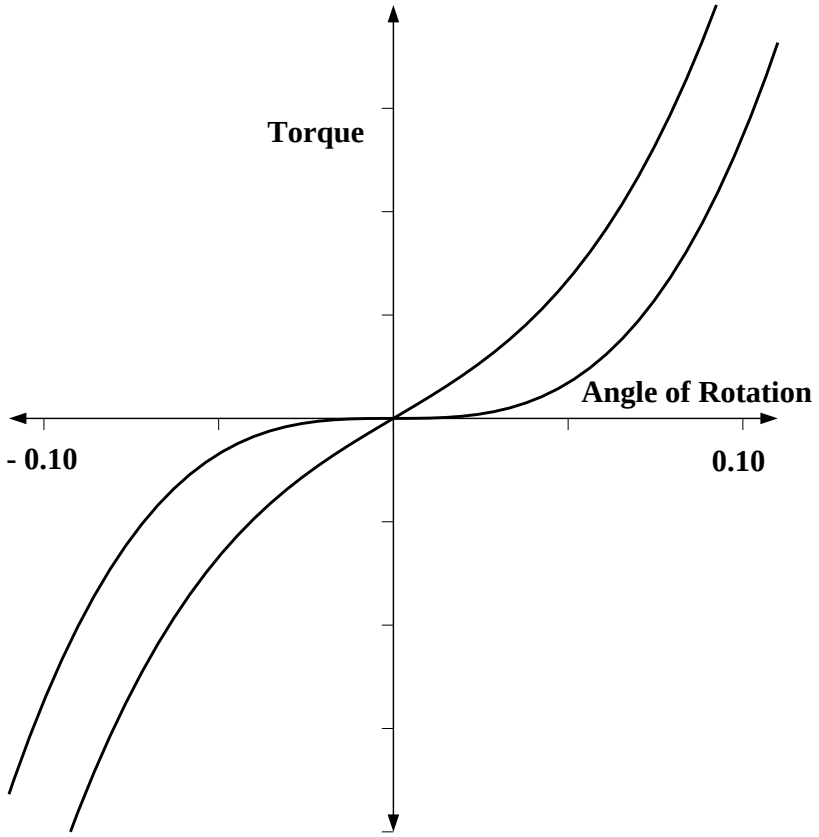

Figure 3. Torque-rotation Response for small Rotations; Prestrains of 0%, 0.2%

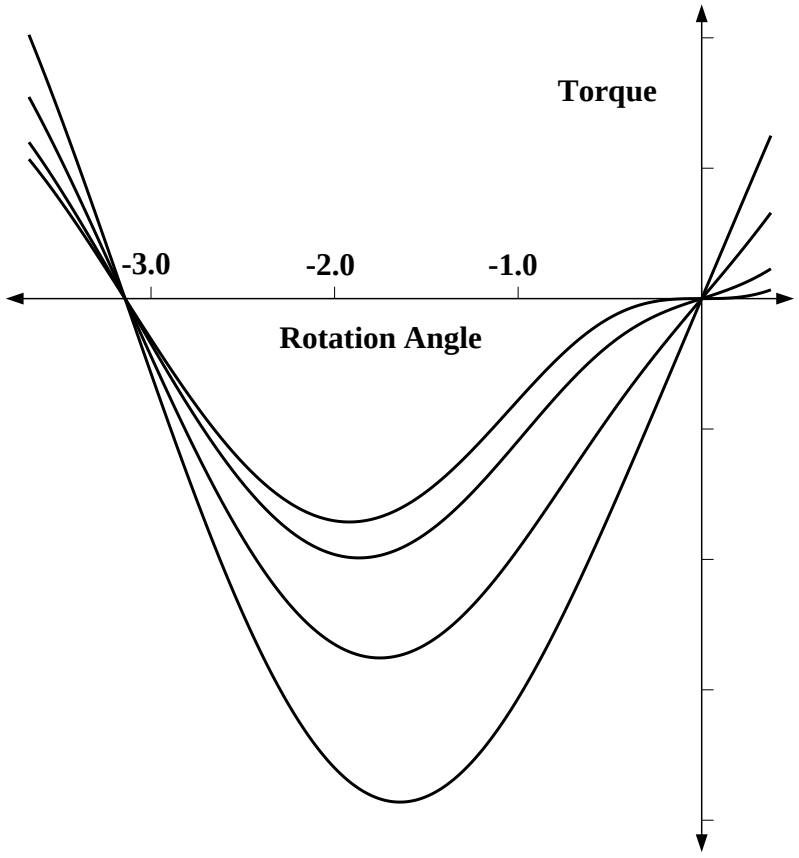

Figure 4. Torque-rotation Response over Feasible Range; Prestrains of 0%, 10%, 50%, and 300%

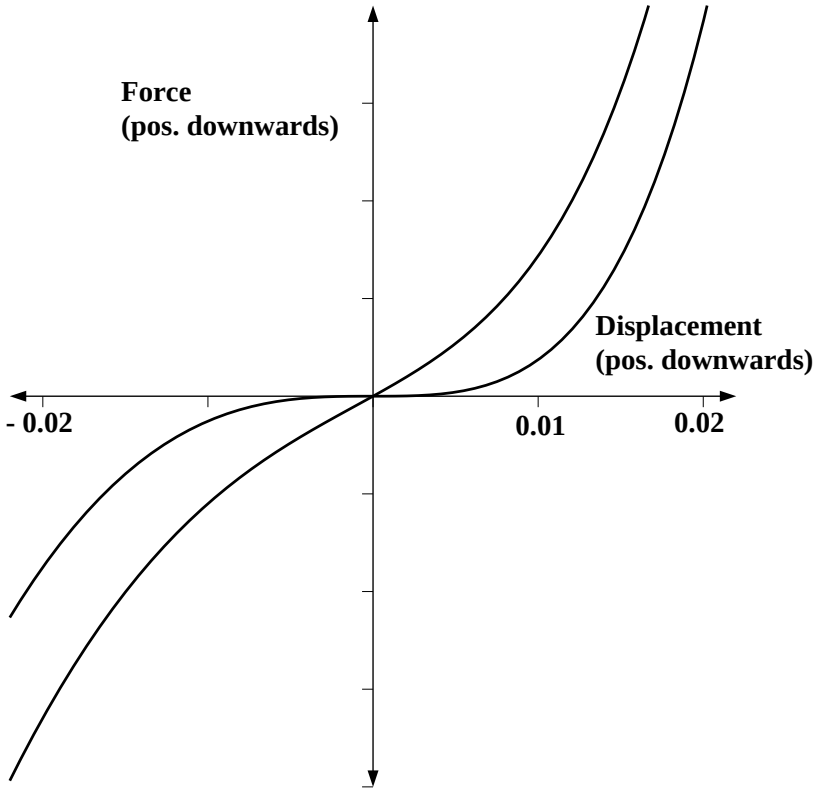

Figure 5. Force-displacement Relations for a Downwards Force; No Prestress and Small Prestress

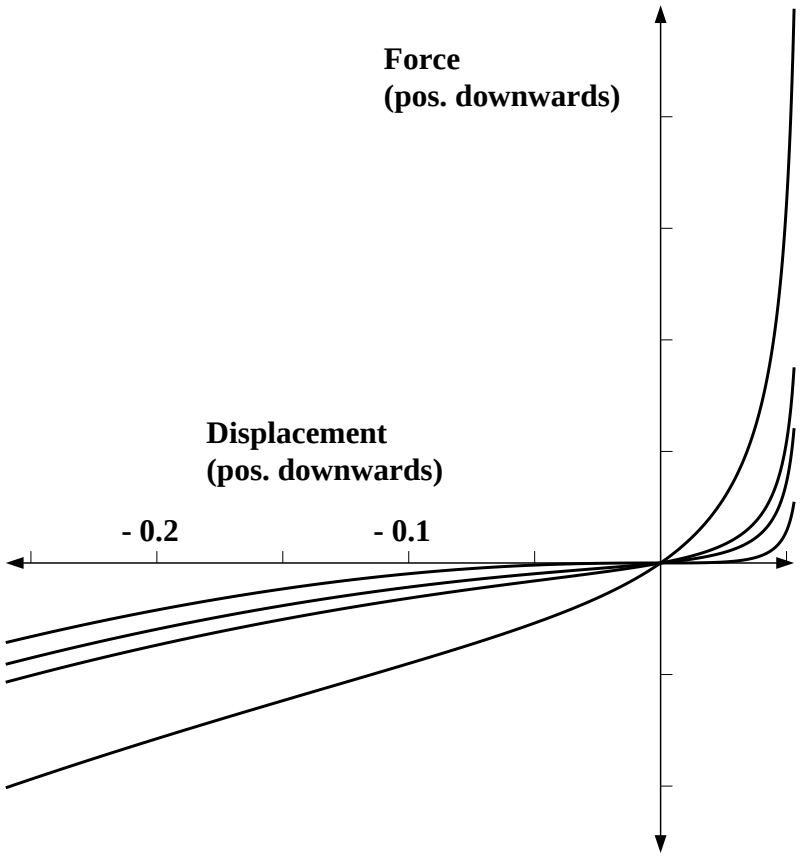

Figure 6. Force-displacement Relations for a Downwards Force; Various Prestresses

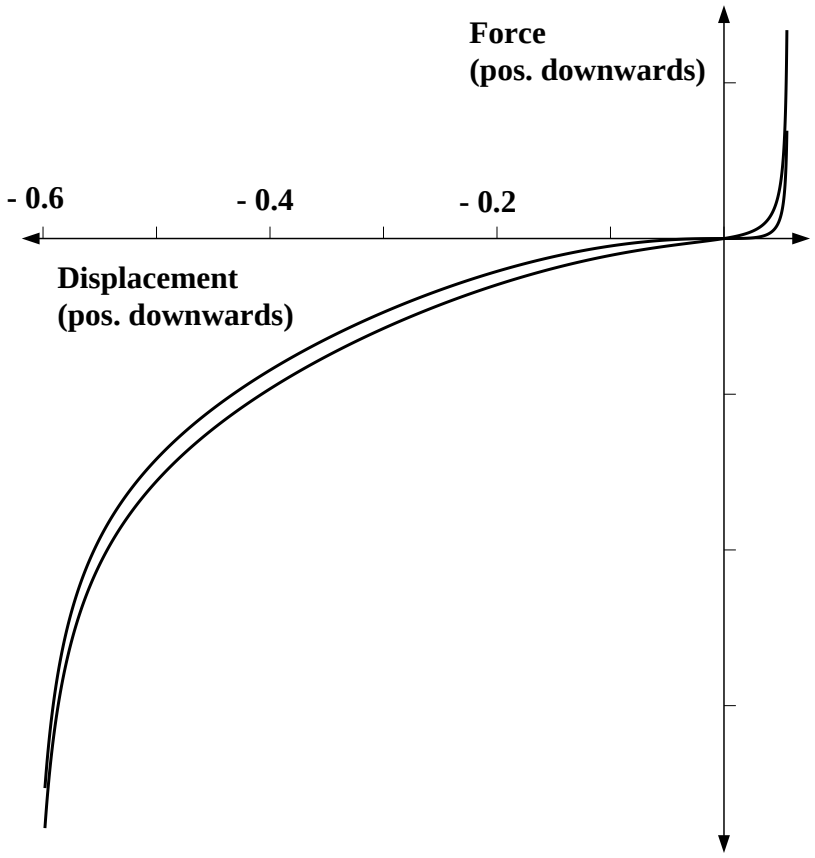

Figure 7. Force-displacement Relations for a Downwards Force; Zero and Large Prestress

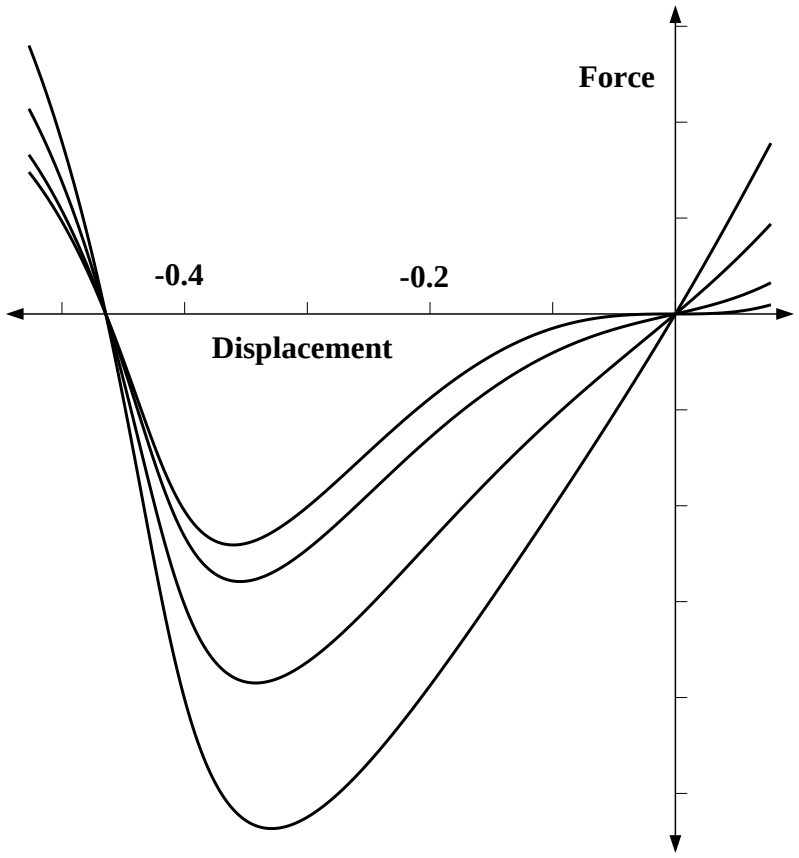

Figure 8. Force-displacement Relations for a Natural-mode Force under Various Prestresses